

higher pressures by three frequently used melting relations: the two empirical relations by Simon and Kraut-Kennedy and the quasi-theoretical melting criterion by Lindemann (6) (Fig. 4). We estimate that the melting temperature of (Mg,Fe)SiO₃-perovskite at the core-mantle boundary (CMB) is between 7000 and 8500 K. This temperature and the melting curve are also significantly higher than well-accepted temperatures of the lower mantle geotherms (Fig. 4).

Most likely, the melting temperature of the lower mantle is not substantially below that of perovskite, because perovskite melts near the eutectic of the Mg-Fe-Si-O system (4), which represents lower mantle chemistry. If this conclusion holds, the extremely large difference between the temperature of the lower mantle and the melting temperature of perovskite has some important geophysical and geochemical implications: (i) Large-scale melting and chemical differentiation of the lower mantle resulting from formation and separation of a melt can be excluded, even if the Earth was significantly hotter in past geologic times. (ii) The temperature dependence of physical properties related to the shear modulus such as viscosity and anelasticity scale with the homologous temperature, T/T_m . The data suggest that the dependence is most reduced in the lower mantle, because this value decreases significantly with depth. (iii) The high melting temperatures of perovskite allow the existence of a large thermal boundary across the D region between mantle and core (7). (iv) Large lateral seismic velocity anomalies in the lower part of the mantle, found from seismic tomography, may result from large variations in temperature (8) because such variations would not necessarily result in partial melting or large decreases in the viscosity.

REFERENCES AND NOTES

- D. L. Heinz and R. Jeanloz, *J. Geophys. Res.* **92**, 11437 (1987); E. Knittle and R. Jeanloz, *Geophys. Res. Lett.* **16**, 421 (1989); J. S. Sweeney and D. L. Heinz, *ibid.* **20**, 855 (1993). The YAG-laser beam, used in these experiments, had to be tightly focused because of the low optical absorption and the lack of a thermally insulating pressure medium. This produced a complicated three-dimensional temperature distribution with extremely large temperature (and pressure) gradients in the polycrystalline sample, which served as its own pressure medium. This situation did not allow a direct measurement of the temperature in the center of the hot spot and temperatures had to be calculated from the measured average temperatures. Melting was not directly detected; instead isotropic optical behavior subsequent to quenching, and indirect thermal analysis were used as the melting criteria.
- E. Ohtani, *Phys. Earth Planet. Inter.* **33**, 12 (1983); J. P. Poirier, *ibid.* **54**, 364 (1989); L. Stixrude and M. S. T. Bukowski, *J. Geophys. Res.* **95**, 19311 (1990).
- M. Matsui and G. D. Price, *Nature* **351**, 735 (1991); B. Kapusta and M. Guillope, *Phys. Earth Planet. Inter.* **75**, 205 (1993).
- E. Ito and T. Katsura, in *High-Pressure Research: Application to Earth and Planetary Sciences*, Y. Syono and M. H. Manghnani, Eds. (TERRAPUB, Tokyo/American Geophysical Union, Washington, DC, 1992), pp. 315–322; T. Kato and M. Kumazawa, *Nature* **316**, 803 (1985). The maximum pressures in these experiments were 250 and 200 kbar, respectively. Use of thermocouples at these pressures leads to an uncertainty in temperature of at least ± 100 K.
- R. Boehler and A. Chopelas, *Geophys. Res. Lett.* **18**, 1147 (1991); in *High-Pressure Research: Application to Earth and Planetary Sciences*, Y. Syono and M. H. Manghnani, Eds. (TERRAPUB, Tokyo/American Geophysical Union, Washington, 1992), pp. 55–60. The three essential features of this laser-heating technique are CO₂-laser radiation, an argon pressure medium, and thin section samples. The high power of CO₂-lasers, the high absorption of its radiation by minerals, the low thermal conductivity of argon, and the small sample thickness, reduce both radial and axial temperature gradients. Temperatures were measured in situ from the center of the hot spot from areas with 3 to 5 μ m in diameter, using a Planck radiation function and solving for both temperature and emissivity, assuming wavelength-independent emissivities. This assumption is probably reasonable for transparent minerals in the spectral range of 530 to 830 nm used in the present measurements. Corrections similar to the known emissivity-wavelength-temperature functions for metals would decrease temperatures by about 100 K at 3000 K and 350 K at 5000 K. Other uncertainties in the temperature measurements, associated with radial or axial temperature gradients, optical geometry, chromatic aberration, and curve fitting add up to less than 100 K in this experiment. The method does not require any correction of the directly measured temperature. Pressures were measured from ruby chips, distributed throughout the pressure cell. Thermal pressures in the melting experiments were small because of the small volume ratios between sample and the argon pressure medium.
- The Simon equation [F. Simon and G. Glatzel, *Z. Anorg. Allg. Chem.* **178**, 309 (1929)] is a power-law relationship between pressure and melting temperature that describes the low-pressure melting behavior of a number of substances reasonably well. The Kraut-Kennedy relation is an empirical linear dependence of the melting temperature, T_m , and the volume, based on observations made on the highly compressible alkali metals [E. A. Kraut and G. C. Kennedy, *Phys. Rev. Lett.* **16**, 608 (1966)]. It has been recently found to describe well the melting behavior of a number of metals and oxides to high compression [R. Boehler, *Earth Planet. Sci. Lett.* **111**, 217 (1992)]. The Lindemann relation [F. A. Lindemann, *Phys. Z.* **11**, 609 (1910)] states that melting occurs when the vibrational amplitude of the atoms (or molecules) reaches a critical fraction of the interatomic distance. This melting relation was used in the form $d \ln T_m / d \ln \rho = 2(\gamma - 1/3)$, where ρ is the density, and γ is the Grüneisen parameter. The pressure dependence of γ was taken from systematics found in direct measurements of the Grüneisen parameter of a large number of materials by R. Boehler and J. Ramakrishnan [*J. Geophys. Res.* **85**, 6996 (1980)], as $d \ln \gamma / d \ln \rho = 1.3 \pm 0.3$.
- R. Boehler [*Nature* **363**, 534 (1993)] estimated a minimum temperature increase across the core-mantle boundary of 1300 K from static melting experiments of iron and iron-oxygen compounds to 2 Mbar.
- D. A. Yuen, O. Cadek, A. Chopelas, and C. Matyska [*Geophys. Res. Lett.* **20**, 899 (1993)] calculated lateral temperature variations, δT , from the measured seismic anomalies, $\delta v/v$ [W.-J. Su and A. M. Dziewonski, *Phys. Earth Planet. Inter.* **74**, 29 (1992)], and new measurements of sound velocities of several minerals at mantle pressures, and pressure systematics of the thermal expansion coefficient, α , using $\delta T = (\delta v/v)(d \ln \rho / d \ln v) \alpha$. Their values of δT are still uncertain, but show a trend toward high-temperature anomalies in excess of 1000 K.
- We thank A. Chopelas and D. Yuen for helpful discussions and A. Chopelas for constructive comments on the manuscript.

6 July 1993; accepted 1 September 1993

3.4-Billion-Year-Old Biogenic Pyrites from Barberton, South Africa: Sulfur Isotope Evidence

Hiroshi Ohmoto,* Takeshi Kakegawa, Donald R. Lowe

Laser ablation mass spectroscopy analyses of sulfur isotopic compositions of microscopic-sized grains of pyrite that formed about 3.4 billion years ago in the Barberton Greenstone Belt, South Africa, show that the pyrite formed by bacterial reduction of seawater sulfate. These data imply that by about 3.4 billion years ago sulfate-reducing bacteria had become active, the oceans were rich in sulfate, and the atmosphere contained appreciable amounts ($> > 10^{-13}$ of the present atmospheric level) of free oxygen.

Sulfate is the second most abundant anion in present-day seawater. It is generated primarily on land by weathering of SO₄²⁻ minerals and pyrite (FeS₂) under an O₂-bearing atmosphere and is transported by rivers to the oceans where it is converted to

SO₄²⁻ minerals, chiefly by evaporation of seawater, and to pyrite. The pyrite forms mostly in normal marine sediments where SO₄²⁻ supplied from the overlying seawater is converted to H₂S (that is, reduction of S⁶⁺ to S²⁻) by SO₄²⁻-reducing bacteria (SRB); the H₂S reacts with Fe-bearing minerals in the sediments to form pyrite. After burial, lithification, metamorphism, and uplift, exposure of marine sedimentary rocks to air generates SO₄²⁻. The present-day cycles of sulfur in the Earth, therefore, are controlled by the presence of free O₂ in

H. Ohmoto and T. Kakegawa, Department of Geosciences, The Pennsylvania State University, University Park, PA 16802, and Institute of Mineralogy, Petrology, and Economic Geology, Tohoku University, Sendai 980, Japan.
D. R. Lowe, Department of Geology, Stanford University, Stanford, CA 94305.

the atmosphere and of SRB in the oceans.

The biogenic pyrites in modern marine sediments typically have highly variable ratios of sulfur isotopes; $\delta^{34}\text{S}$ values (1) range from about -50 to $+10$ per mil (2). In contrast, the $\delta^{34}\text{S}$ values of pyrites from sedimentary rocks of Archean age [>2.5 billion years ago (Ga)] fall generally in a narrow range of 0 ± 5 per mil (3); they are essentially identical to those for sulfides in normal igneous rocks. Hence, many investigators (3) have suggested that pyrite in Archean sedimentary rocks formed from H_2S derived from magmas rather than by bacterial reduction of seawater SO_4^{2-} . The implications have been that, before ~ 2.5 Ga, SRB had not evolved, the oceans were free of SO_4^{2-} , and the atmosphere contained virtually no free O_2 . However, some investigators (3) have interpreted the same sulfur isotope data differently. They have suggested that most pyrites in Archean sedimentary rocks were also formed by SRB; the differences in their isotopic characteristics from the modern biogenic pyrites would have been caused primarily by differences in environmental parameters for SRB, such as the SO_4^{2-} content and temperature of seawater.

One reason for the ambiguity of sulfur isotope data is that the analyses were performed on bulk multi-grain chemical or mechanical separates from hand specimens, most ~ 100 cm^3 or larger, rather than on single grains because the conventional analytical techniques required a large amount (>5 mg; ~ 1000 crystals of ~ 100 μm in size) of sulfide minerals. This approach homogenizes isotopic variations. Highly sensitive mass spectrometers and recent developments in laser technology have made it possible to determine the $\delta^{34}\text{S}$ value of a single sulfide crystal, ~ 150 μm or larger in diameter (4–6). We used these techniques to examine isotopic variations among individual microscopic grains of pyrite in a small volume (<10 cm^3) of rock.

We sampled a shale and three black (organic carbon-rich) cherts from four locations in an approximately 10 km by 20 km area of the Barberton Greenstone Belt, South Africa (7). These rocks all belong to the uppermost unit (~ 100 m thick) of the upper Onverwacht Group (age of about 3.4 to 3.3 Ga); this unit is overlain by the Fig Tree Group that has an age of 3.26 to 3.22 Ga (7). The sulfide minerals in the four samples are almost exclusively pyrite, euhedral to subhedral in shape. The pyrites in the cherts are about 50 to 250 μm in diameter, but those in the shale are about 0.5 to 3.0 mm in diameter. They are disseminated throughout the rocks but are typically concentrated in ~ 1 - to ~ 5 -mm thick layers paralleling bedding. No veins or veinlets containing sulfide minerals were observed. These features suggest that most of the pyrites formed during or shortly after deposition of the host sediments on the sea floor.

We attempted initially to analyze the $\delta^{34}\text{S}$ values of microscopic grains of pyrite in the sedimentary rocks in situ. This attempt was abandoned, however, because laser ablation of sedimentary rocks, which typically contain more carbon-bearing compounds (kerogen) than sulfides, produces a variety of hydrocarbon gases that interfere with the isotopic analysis of the SO_2 generated from sulfide minerals. Therefore, we analyzed single grains of pyrite, about 150 μm to 1 mm in size, that were separated physically from the rocks smaller than 10 cm^3 . The pyrite grains were mounted individually on a gold plate and were ablated by a Nd-YAG laser in an O_2 atmosphere. The vaporized sulfide reacted with the O_2 to form SO_2 that was introduced to a VG Prism II mass spectrometer for sulfur isotope analysis. The uncertainty in the $\delta^{34}\text{S}$ values is typically ± 0.3 per mil.

We analyzed a total of 123 grains of pyrite from the four rock samples. The $\delta^{34}\text{S}$ values ranged from -3.0 to $+8.6$ per mil (that is, a variation of ~ 12 per mil) with a mean of $+1.1$ per mil. We observed a variation of up to 10 per mil among pyrites from a single ~ 10 - cm^3 rock specimen (Fig. 1C); this variation is greater than the 7 per mil variation ($\delta^{34}\text{S} = -4$ to $+3$ per mil) reported by earlier investigators (3) on 23 samples of bulk sulfide minerals from the various stratigraphic sections in the Barberton Greenstone Belt.

Some of the large (>150 μm) crystals investigated in this study may have formed through dissolution and recrystallization of smaller crystals during deep burial and metamorphism of the sedimentary rocks. The rocks are of the lower greenschist facies, suggesting metamorphic temperatures up to a few hundred degrees Celsius. Recrystallization of smaller crystals into larger ones homogenizes their isotopic compositions (8). Therefore, the $\delta^{34}\text{S}$ variations among the original (early diagenetic) pyrite crystals in these samples

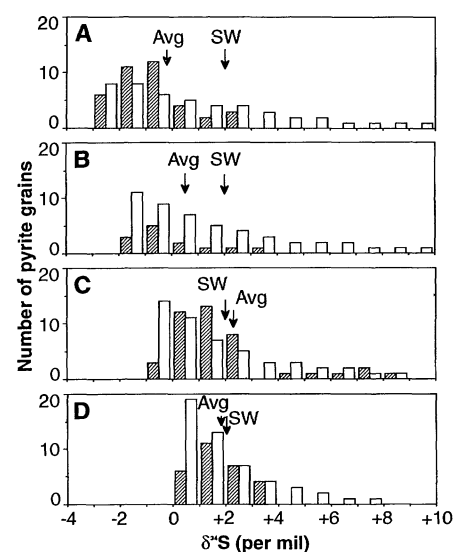
were probably greater than those observed today: >4 per mil in the shale and >6 to 10 per mil in the cherts.

The dominant igneous activity in the Earth during the Archean was basaltic volcanism under submarine environments. The dominant sulfur-bearing species in volcanic gases and hydrothermal fluids derived from basaltic magmas is H_2S when the total fluid pressure is greater than ~ 100 bars (8); its $\delta^{34}\text{S}$ value falls in a narrow range of $+1 \pm 1$ per mil (8). If the Archean oceans contained magmatic H_2S , its $\delta^{34}\text{S}$ value must also have been within the range of $+1 \pm 1$ per mil. The common occurrence of pyrites in the studied samples with $\delta^{34}\text{S}$ values outside this range indicates that the pyrites did not form from magmatic H_2S , either directly or indirectly.

Modern submarine hydrothermal fluids, discharging on mid-ocean ridges at about 100° to 400°C , appear from their oxygen and hydrogen isotopic characteristics to be primarily heated seawater rather than magmatic fluids (9). During the circulation of these fluids through hot rocks, SO_4^{2-} in the seawater may be reduced to H_2S nonbiologically, for example, by reaction with Fe^{2+} -bearing minerals (9). Walker and Brimblecombe (10) have suggested that sulfides in Archean sedimentary rocks may have formed by such a process.

Normal seawater ~ 3.4 Ga apparently contained some SO_4^{2-} with a $\delta^{34}\text{S}$ value around $+2$ per mil (3), because SO_4^{2-} minerals in about 3.5 to 3.3 Ga sedimentary rocks in different parts of the world have similar minimum $\delta^{34}\text{S}$ values ($\sim +3.0$ per mil), and because there exists an ~ 1 per mil isotopic fractionation between SO_4^{2-} minerals and SO_4^{2-} at around 25°C (2). The hydrothermal H_2S produced by nonbiologic reduction of Archean seawater SO_4^{2-} may have had $\delta^{34}\text{S}$ values anywhere between ~ -30 and $\sim +2$ per mil, depend-

Fig. 1. Comparisons of the $\delta^{34}\text{S}$ frequency diagrams for single grains of pyrite crystals for samples from three black cherts (A, B, and C) and one shale (D) from the Barberton Greenstone Belt, South Africa (shaded columns), with those predicted from a theoretical model (open columns). Avg is the average $\delta^{34}\text{S}$ value for the analyzed pyrite grains and SW is the estimated $\delta^{34}\text{S}$ value for SO_4^{2-} in seawater ~ 3.4 Ga (3). (A) Data on sample 186 ($n = 38$) versus the theoretical $\delta^{34}\text{S}$ distribution at $\Delta = 5$ per mil and $n = 50$ (four theoretical points, $\delta^{34}\text{S} = 10, 11, 12,$ and 16 , lie outside of the range). (B) Data on sample 187 ($n = 14$) versus the theoretical values at $\Delta = 4$ per mil and $n = 50$ (two theoretical points, $\delta^{34}\text{S} = 11$ and 13 , lie outside of the range). (C) Data on sample 142 ($n = 43$) versus the theoretical values at $\Delta = 3$ per mil and $n = 50$. (D) Data on sample 296 ($n = 28$) versus the theoretical values at $\Delta = 2$ per mil and $n = 50$.



ing on the degree of SO_4^{2-} reduction; complete conversion of SO_4^{2-} results in H_2S of $\sim +2$ per mil. Some Archean massive sulfide ores that are rich in Zn, Cu, Au, and Ag have $\delta^{34}\text{S}$ values between ~ -15 to $\sim +3$ per mil, suggesting that they formed from hydrothermal H_2S of seawater SO_4^{2-} origin (3). However, the disseminated pyrite grains we analyzed have $\delta^{34}\text{S}$ values as high as $+8$ per mil; these are not likely to have formed from hydrothermal H_2S .

The observed variations in the $\delta^{34}\text{S}$ values among pyrite crystals occurring in a small volume of a sedimentary rock can be explained most easily by models involving bacterial sulfate reduction (BSR). The difference between the $\delta^{34}\text{S}$ value of normal seawater SO_4^{2-} and the minimum $\delta^{34}\text{S}$ value among biogenic pyrite crystals in a sedimentary rock reflects the magnitude of kinetic isotopic effects, $\Delta_{\text{SO}_4\text{-H}_2\text{S}}$, associated with BSR; the $\Delta_{\text{SO}_4\text{-H}_2\text{S}}$ value in modern marine sediments varies regionally from ~ 70 to ~ 20 per mil (2). If all the pyrites that we studied were formed by bacterial reduction of seawater SO_4^{2-} with a $\delta^{34}\text{S}$ value of $\sim +2$ per mil, the minimum $\delta^{34}\text{S}$ values of -3.0 to $+0.2$ per mil for the pyrite crystals (Fig. 1, A through D) suggest that the $\Delta_{\text{SO}_4\text{-H}_2\text{S}}$ values associated with BSR in oceans ~ 3.4 Ga were only ~ 5 to ~ 2 per mil. This suggestion can be tested by comparing other statistics of the $\delta^{34}\text{S}$ frequency diagram for each sample with those predicted from a Rayleigh distillation model (8). In our model computations, all SO_4^{2-} that entered an $\sim 10\text{-cm}^3$ sedimentary rock was successively converted to 50 pyrite crystals of equal size (11).

The $\delta^{34}\text{S}$ frequency diagram for the 43 pyrite grains from sample no. 142 (black chert, Fig. 1C) is in agreement with the theoretical distribution ($n = 50$, $\Delta_{\text{SO}_4\text{-H}_2\text{S}} = 3$ per mil) in the minimum (-1 per mil), the maximum ($+9$ per mil), and the average ($+2$ per mil) $\delta^{34}\text{S}$ and with the trend of decreasing occurrences of pyrites with higher $\delta^{34}\text{S}$ values. Some discrepancies exist but they are not serious. For example, the maximum $\delta^{34}\text{S}$ values for the other three samples are less than the predicted values (Fig. 1, A, B, and D); the discrepancies may have resulted from the much smaller number of pyrite grains analyzed compared with that ($n = 50$) used in the model computations. In the model computations, the peak and the minimum $\delta^{34}\text{S}$ values coincide; in the analyzed samples, the peak $\delta^{34}\text{S}$ values are higher than the minimum $\delta^{34}\text{S}$ values by a few per mil. Such a relation suggests that $\sim 10\text{-cm}^3$ blocks of sediment did not represent simple closed systems with respect to SO_4^{2-} , and that SO_4^{2-} reduction and sulfide formation likely continued while the sediment was buried to depths of greater than ~ 10 cm from the sea floor.

Two different models may be considered to explain the $\Delta_{\text{SO}_4\text{-H}_2\text{S}}$ values of ~ 5 to ~ 2 per mil accompanying BSR in the Archean oceans, in contrast with the values of ~ 70 to ~ 20 per mil in modern oceans. The first model [for example (10)] is that the SO_4^{2-} content of seawater ~ 3.4 Ga was less than or equal to $\sim 1/30$ the present value of 3×10^{-2} mol/liter ($< 10^{-3}$ mol/liter). The second model (12) is that the SO_4^{2-} content of the Archean oceans was greater than or equal to $\sim 1/3$ the present level ($\geq 10^{-2}$ mol/liter), but the activity of SRB was much higher than in the modern oceans. Both models are consistent with the available laboratory data for sulfur isotope fractionation by SRB (3). However, the isotopic and other geochemical data for Archean massive sulfide ores, which appear to have formed from the mixing of normal seawater with hydrothermal fluids of seawater origin, can be better explained if the SO_4^{2-} content of Archean seawater was $\sim 10^{-2}$ mol/liter (3).

If the relation between the rates of SO_4^{2-} reduction and the $\Delta_{\text{SO}_4\text{-H}_2\text{S}}$ values observed in modern marine sediments is applicable to SRB in Archean oceans, the $\Delta_{\text{SO}_4\text{-H}_2\text{S}}$ values of ~ 5 to ~ 2 per mil suggest that the rates of BSR in marine sediments in the Barberton district ~ 3.4 Ga were ~ 10 to ~ 100 mol/liter per year (Fig. 2). Such rates are about two to five orders of magnitude higher than those observed in normal marine sediments today but are comparable to the highest rate observed in algal mats of the Solar Lake, Sinai (13).

The higher rates of SO_4^{2-} reduction in Archean oceans could have been achieved under a CO_2 -rich atmosphere because the CO_2 content in the atmosphere influences the two most important parameters that control the rate of SO_4^{2-} reduction: temperature and the availability of digestible organic matter to SRB in oceans (3). Ac-

cording to Walker and Brimblecombe (10), a SO_4^{2-} content of less than or equal to $\sim 1/30$ the present seawater concentration may be produced by photochemical reactions involving volcanogenic SO_2 in an atmosphere containing virtually no free O_2 ($\sim 10^{-13}$ of the present atmospheric level), but concentrations above that require the presence of appreciable amounts of free O_2 in the atmosphere. The results of this study imply that the geochemical cycle of sulfur in near surface environments has been virtually unchanged since at least ~ 3.4 Ga.

REFERENCES AND NOTES

1. Defined as
2. H. Ohmoto, C. J. Kaiser, K. A. Geer, in *Stable Isotopes and Fluid Processes in Mineralization*, H. K. Herbert and S. E. Ho, Eds. (University of Western Australia, Perth, 1990), pp. 70-120.
3. For a review of sulfur isotope data on Archean sedimentary rocks and of the various interpretations, see H. Ohmoto, in *Early Organic Evolution: Implications for Mineral and Energy Resources*, M. Schidlowski et al., Eds. (Springer-Verlag, Berlin, 1992), pp. 378-397.
4. L. M. Jones et al., *Terra Cognita* 6, 263 (1986).
5. S. P. Kelley and A. E. Fallick, *Geochim. Cosmochim. Acta* 54, 883 (1990).
6. D. E. Crowe et al., *ibid.*, p. 2075.
7. D. R. Lowe and P. R. Knauth, *J. Geol.* 85, 699 (1977).
8. H. Ohmoto and R. O. Rye, in *Geochemistry of Hydrothermal Ore Deposits*, H. L. Barnes, Ed. (Wiley, New York, ed. 2, 1979), pp. 509-567.
9. H. Ohmoto, in *Stable Isotopes in High Temperature Geological Processes*, J. E. Valley et al., Eds. (American Mineralogical Society, Washington, DC, 1986), pp. 491-560.
10. J. C. G. Walker and P. Brimblecombe, *Precambrian Res.* 28, 205 (1985).
11. In a system closed to SO_4^{2-} , the $\delta^{34}\text{S}$ value of a pyrite crystal formed at a specific time can be computed from the following Rayleigh distillation equation (8)
12. H. Ohmoto and R. P. Felder, *Nature* 328, 244 (1987).
13. B. Jørgensen and Y. Cohen, *Limnol. Oceanogr.* 22, 657 (1977).
14. Supported by grants to H.O. from NSF (EAR-9003554) and from the Japanese Ministry of Science, Education, and Culture (03102002) and by grants to D.R.L. from the National Aeronautics and Space Administration Exobiology Program (NCA2-332) and NSF (EAR-89-04830). We thank M. Mitchlick, D. P. Walizer, K. Hayashi, and Y. Watanabe for technical assistance and I. N. MacInnis, T. Kato, L. M. Kump, J. F. Kasting, and the two anonymous reviewers for useful suggestions.

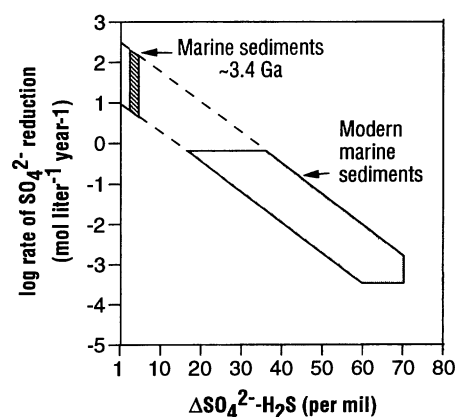


Fig. 2. The observed relation between the rates of BSR and the magnitudes of kinetic isotope effects ($\Delta_{\text{SO}_4\text{-H}_2\text{S}}$) in modern marine sediments (3) and the estimated rates of BSR in the oceans ~ 3.4 Ga.

1 June 1993; accepted 4 August 1993